NUMERICAL INVESTIGATION OF EVAPORATION OF
NONLINEAR MULTICOMPONENT VOLATILE SOLUTIONS
FROM A CAPILLARY

P. S. Kuts, V. I. Astapova,
and S. Yu. Kalinin

A mathematical experiment is conducted on the mechanism of evaporation of a ternary volatile solution from a cylindrical capillary.

In real materials, a liquid which cannot be driven off is a solution of complex composition. Often all the components of the solution can change from one phase to another. Recently many works have been published in which the evaporation of such liquids is examined. The vacuum evaporation model of a binary solution, both components of which are volatile, is presented in [1]. The authors analyzed the model for various limiting cases. The theory of evaporation of volatile solutions from capillaries into air is developed in [2-4]. The evaporation mechanism for volatile multicomponent mixtures is complex because the mixture composition changes during evaporation due to rapid evaporation of the more volatile components. Moreover, component concentrations in the evaporation boundary differ from those in the volume of the mixture. A theoretical evaporation rate of a binary volatile solution from a capillary has been calculated [2-4] without considering the change in component concentrations at the evaporation boundary. An analytical expression has been obtained [4] for calculating the concentration change at the evaporation boundary of a binary solution in the case of a semi-infinite capillary. The author assumes that the evaporation kinetics qualitatively correspond to the evaporation of a pure liquid.

We have developed a numerical method to calculate the time-dependent evaporation rate and concentration profiles of the liquid-phase components of a multicomponent volatile solution as a function of the change in the concentrations at the phase change boundary.

We consider a right cylindrical capillary, filled with an n-component volatile solution. The Ox-axis is pointed from the bottom of the capillary to its mouth. We will assume that evaporation occurs at constant pressure and temperature into an inert gas medium. We will further assume that mass transfer to the evaporation boundary occurs by diffusion. Because the diffusion relaxation time in the gas phase is small compared to the evaporation time, we will assume that the vapor flows of components in the gas phase are at equilibrium for any position of the moving evaporation boundary.

If diffusion in the liquid phase is considered, the system of equations and boundary conditions for describing isothermal evaporation of a multicomponent mixture has the form:

$$\frac{\partial \rho_i(x, t)}{\partial t} = \frac{\partial}{\partial x} \left(D_i(\rho_1, \ldots, \rho_n) \frac{\partial \rho_i(x, t)}{\partial t} \right) (0 \leqslant x \leqslant l, \; i = 1, \ldots, n), \tag{1}$$

$$\rho_i(x, 0) = \rho i_0, \quad \frac{\partial \rho_i(0, t)}{\partial x} = 0, \tag{2}$$

$$- D_i(\rho_1, \ldots, \rho_n) \frac{\partial \rho_i(l, t)}{\partial x} = G_i(\rho_i(l, t)) - \rho_i(l, t) \frac{\sum\limits_{j=1}^{n} G_j(\rho_j(l, t))}{\sum\limits_{j=1}^{n} \rho_j(l, t)}, \tag{3}$$

$$\frac{dl}{dt} = -\sum_{j=1}^{n} \frac{G_j(\rho_j(l, t))}{\rho_j^0}.$$ (4)

The expression for the evaporation boundary condition (3) is derived [4] under the assumption of diffusion flow of the mixture components to a moving evaporation boundary. The continuity of mass flow through the boundary is used in the derivation. The displacement of the evaporation boundary [4] is obtained [2, 3] from the mass-conservation law for each component and under the assumption that the volumes of the miscible components are combined additively.

The expressions for the vapor flux G_i of the components at temperatures less than the boiling point for the mixture and for a constant pressure in the capillary are determined from a system of equations [5] with the assumption that air molecules cannot penetrate the evaporation boundary ($G_{n+1} = 0$):

$$c_i \frac{kT}{P} \sum_{\substack{j=1 \\ j \neq i}}^{n} \frac{G_j}{D_{ij}' m_j} - \frac{G_i kT}{m_i P} \sum_{\substack{j=1 \\ j \neq i}}^{n+1} \frac{c_j}{D_{ij}'} = \frac{dc_i}{dx},$$ (5)

$$c_{n+1} \frac{kT}{P} \sum_{j=1}^{n} \frac{G_j}{D_{j(n+1)}' m_j} = \frac{dc_{n+1}}{dx},$$ (6)

where $c_i = P_i/P$.

The boundary conditions to (5) and (6) have the form

$$c_i(l) = c_{il},$$ (7)

$$c_i(L) = c_{iL}.$$ (8)

The dependence of the vapor concentration of the i-th component at the evaporation boundary on the concentration of the i-th component in the liquid phase is characterized by the Raoult—Henry law for ideal solutions. For real solutions the quantitative measure of the deviation from the ideal is the activity coefficient γ_i of the i-th component. Then the equation relating c_{il} and $\rho_i(l, t)$ takes the form

$$c_{il} = \gamma_i \frac{P_{is}^0}{P} X_{il},$$ (9)

$$X_{il} = \frac{\rho_i(l, t)/\mu_i}{\sum_{j=1}^{n} \rho_j(l, t)/\mu_j}.$$ (10)

The problem (1)-(4) is related to problems with a moving boundary and is highly nonlinear. It was solved numerically for ternary mixtures using the method of approximations for mixed problems for a quasi-linear parabolic equation [6]. For a fixed value of l the distributions of liquid-phase component concentrations along the Ox-axis in the segment [0, l] were found from the system of equations (1) with the boundary conditions (2) and (3) using the standard PKNG program [6]. The values of $G_i\{\rho_i(l, t)\}$ were determined from (1) and the boundary conditions (5)-(8) using an algorithm derived from the Runge-Kutta numerical integration method. After the concentration distributions were found, $G_i\{\rho_i(l, t)\}$ was calculated for all components and Eq. (4) was solved. The new value of l from (4) was found by trapezoidal integration, because the experimental curves of $l = f(\sqrt{t})$ are smooth, and because the integration time step was chosen much less than the length of the process. The resultant segment [0, l] was decomposed into the same number of steps in X, and the concentrations of all components were found at the new nodes by integration. The standard program KINPS [7] was used for interpolation.

The algorithm presented above was used to compute the evaporation rate of a ternary mixture of acetone—cyclohexanone—toluene from a cylindrical capillary into air. The concentrations of the components were obtained at the evaporation boundary during the whole process. The liquid and gas-phase concentrations along the Ox-axis were found as functions of time. The diffusion coefficients in the liquid and gas phases were found from recommendations in [8]. The saturated vapor pressures were calculated from Antoine's equation, and the activity coefficients γ_i were calculated from the UNIFAC method [8].

The resultant calculated displacements of the evaporation boundary $\Delta l = L - l$ as a function of time were compared with experimental data (Fig. 1). The experiment was conducted
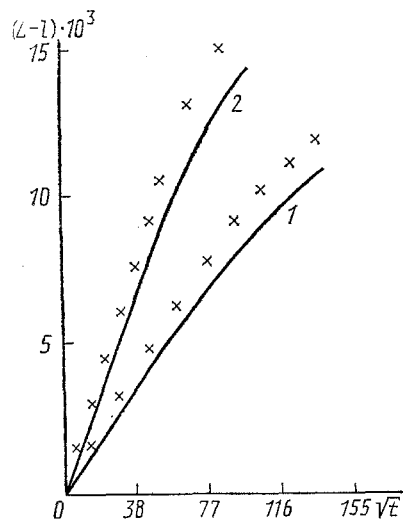
Fig. 1

Fig. 2

Fig. 1. Displacement of the evaporation boundary $(L - \ell)$ vs. time for a mixture of acetone $(\rho_{10} = 203$ kg/m$^3)$, cyclohexanone $(\rho_{20} = 343$ kg/m$^3)$, and toluene $(\rho_{30} = 332$ kg/m$^3)$: 1) T = 330 K; 2) T = 358 K; points show experimental values. $(L - \ell)$ is in meters; t in seconds.
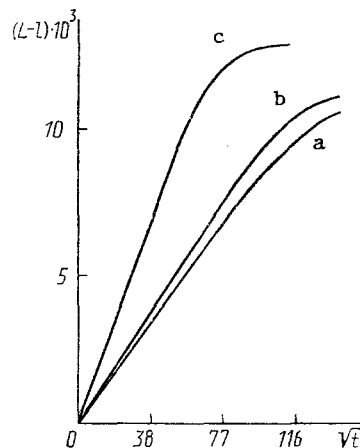
Fig. 2. Displacement of the evaporation boundary vs. time for a mixture of acetone, cyclohexanone, and toluene at T = 330 K. a) $\rho_{10} = 203$ kg/m^3, $\rho_{20} = 343$ kg/m^3, and $\rho_{30} = 332$ kg/m^3; b) $\rho_{10} = 395$ kg/m^3, $\rho_{20} = 342$ kg/m^3, and $\rho_{30} = 121$ kg/m^3; c) $\rho_{10} = 553$ kg/m^3, $\rho_{20} = 152$ kg/m^3, and $\rho_{30} = 121$ kg/m^3; (indices: 1), acetone; 2, cyclohexanone, 3, toluene).
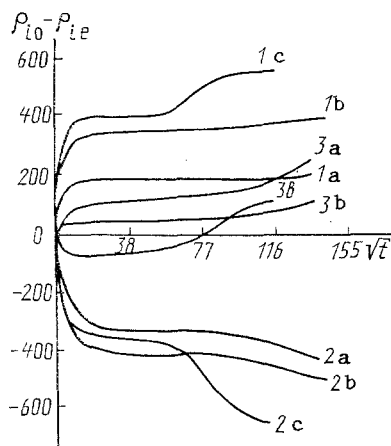

Fig. 3. Change in component concentrations at the evaporation boundary, compared to the initial concentrations $\Delta\rho_{i\ell} = \rho_{i0} - \rho_i$ (ℓ, t) vs. time (T = 330 K): 1) acetone; 2) cyclor hexanone; 3) toluene; a, b, and c are the same as in Fig. 2.

by the method in [9]. As can be seen from Fig. 1, correlation between the experimental and theoretical dependences is good for various process temperatures. The effect of the concentration of the more volatile component on the evaporation rate of the mixture is shown in Fig. 2. As the initial concentration ρ_{10} of the most volatile component (acetone) is increased, the evaporation rate increases, and the section without acetone (curve c) is sharply delineated. The evaporation mechanism of the ternary mixture as a function of the initial acetone concentration ρ_{10} can be followed from Fig. 3. At the very beginning of
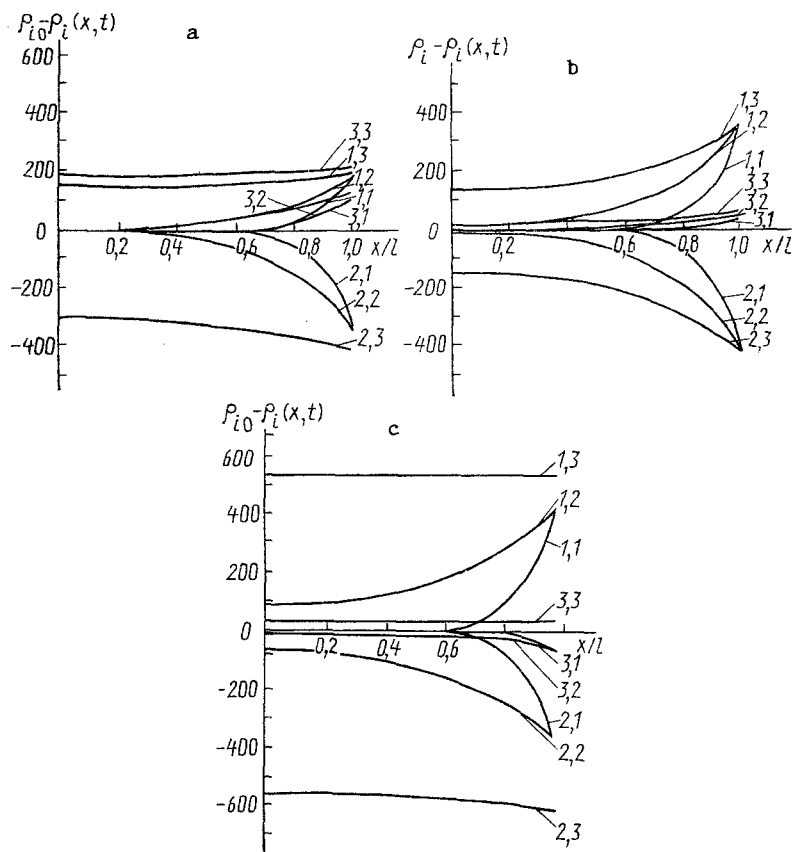
Fig. 4. Change in component concentrations compared to initial values $\Delta\rho_i = \rho_{i0} - \rho_i(x, t)$ vs. x/ℓ for various times ($T = 313$ K; a, b, and c are the same as in Fig. 2): a) 1.1, 1.2, and 1.3 are for acetone at times $\sqrt{t} = 30$, 58, and 124 $\sec^{1/2}$, respectively; 2.1, 2.2, and 2.3 are for cyclohexanone and 3.1, 3.2, and 3.3 are for toluene at the same time; in b) and c) the times are $\sqrt{t} = 30$, 58, and 89 $\sec^{1/2}$.

evaporation, component concentrations, different from the initial concentrations, are established at the phase transition boundary, and the evaporation occurs with practically constant concentrations for some time. The value of $\Delta\sigma_{1\ell} = \rho_{10} - \rho_1(\ell, t)$ increases as ρ_{10} is increased (curves 1a-c). The same figure shows the changes $\Delta\rho_{2\ell}$ (cyclohexanone) and $\Delta\rho_{3\ell}$ (toluene). The length of the segment with constant concentrations decreases as ρ_{10} is increased. Then a segment of evaporation begins with variable concentrations at the boundary. This is shown most clearly for the highest value of ρ_{10} (curves 1c, 2c, and 3c). This interval of time corresponds to a deviation from the linear dependence of $\ell = f(\sqrt{t})$ (see Fig. 2). After the acetone is evaporated, the mixture of cyclohexanone and toluene remain, and the further evaporation follows the mechanism for evaporation of a binary mixture: the concentration of the more volatile component (now toluene) decreases ($\Delta\rho_{3\ell}$ increases), and the concentration of cyclohexanone continues to increase ($\Delta\rho_{2\ell}$ decreases).

The distribution of component concentrations along the depth of the capillary at various times is shown in Fig. 4. At the beginning of the evaporation, the concentrations change only near the evaporation boundary. At later times the concentrations change throughout the whole depth of the solution. Consequently the capillary can be considered semi-infinite only at the initial stage of evaporation. This behavior of the concentration profiles is observed for all investigated initial concentrations; only the deviations from the initial values change (see Fig. 4). Thus, the proposed algorithm using the model (1)-(6) can provide substantial information on the evaporation mechanism of volatile components.

NOTATION

ρ is mass concentration, kg/m^3; t is time; x is the coordinate along the Ox-axis, m; D is the diffusion coefficient, m^2/sec; ℓ is the coordinate of the moving boundary, m; n is the number of mixture components; G is the vapor flux, kg/(m^2·sec); T is temperature, K; k is Boltzmann's constant, k = 1.38·10^{-16} J/deg; P is pressure, Pa; m is the molecular weight, kg; D'_{ij} is the binary diffusion coefficient in the gas phase, m^2/sec; L is the coordinate of the mouth of the capillary, m; γ is the activity coefficient; subscript 0 is for the initial moment of time; superscript 0 is for the pure component; s refers to saturated vapor; n + 1 refers to the external gas.

LITERATURE CITED

1. P. P. Zolotarev, A. A. Zhukhovitskii', and Yu. V. Pokhvisnev, Zh. Fiz. Khim., 57, No. 3, 668-672 (1983).
2. N. I. Gamayunov, L. A. Uvarova, V. L. Malyshev, and A. S. Fel'dblyum, Inzh.-fiz. Zh., 46, No. 3, 442-446 (1984).
3. V. L. Malyshev and L. A. Uvarova, Vestsi SSR, Ser. Fiz.-Énerg. Navuk, No. 1, 90-93 (1985).
4. A. S. Fel'dblyum, "Evaporation of binary liquid mixtures from capillaries at various temperatures," Dissertation for Candidate of Physical—Mathematical Sciences [in Russian], Kalinin (1984).
5. R. Bird, V. Stuart, and E. Lightfoot, Transport Phenomena [Russian translation], Moscow (1974).
6. Computer program warranty No. 41 [in Russian], Inst. Mat., Akad. Nauk B. SSR, Minsk (1982).
7. Computer program warranty No. 11 [in Russian], Inst. Mat. Akad. Nauk B. SSR, Minsk (1976).
8. R. Reed, J. Prausnitz, and T. Sherwood, Properties of Gases and Liquids [Russian translation], Leningrad (1982).
9. S. N. Zotov, Ya. I. Rabinovich, and N. V. Churaev, Inzh.-fiz. Zh., 34, No. 6, 1035-1039 (1978).

FEATURES OF PERIODIC TEMPERATURE PROFILES IN

FILTRATING CAPILLARY POROUS MEDIA

A. A. Lipaev and V. A. Chugunov   UDC 536.251+550.632

The behavior of temperature profiles is examined in filtrating capillary porous media which are subjected to periodic heating. Reasons are described for amplitude shift in the temperature oscillations versus the fluid filtration rate.

The presence of a filtration flow in capillary porous media which are subjected to periodic heating changes their spatial and time-dependent temperature profiles. Thus, a previously unknown relationship was established experimentally [1] between increased heat and mass exchange rates with the earth's surface and increased amplitude of temperature oscillations with depth. This relationship was confirmed by investigations on filtering samples of reservoir rock by imposing periodic heat on one of its ends and measuring the periodic components of the temperature near the other [2]. Here in particular it was found that the amplitude of the temperature oscillations depended on the dimensionless filtration rate in a complex fashion. Thus, if the filtration and heat flows are in the same direction, the amplitude of the temperature oscillations will have a maximum at a given point in the porous medium, which maximum depends on the frequency of the imposed heat flow.